

# Effect of contact angle hysteresis on the removal of the sporelings of the green alga *Ulva* from the fouling-release coatings synthesized from polyolefin polymers

Ikrim O. Ucar, C. Elif Cansoy, and H. Yildirim Erbil<sup>a)</sup>

Department of Chemical Engineering, Gebze Institute of Technology, Cayirova, Gebze 41400, Kocaeli, Turkey

Michala E. Pettitt, Maureen E. Callow, and James A. Callow

School of Biosciences, University of Birmingham, Birmingham B15 2TT, United Kingdom

(Received 18 June 2010; accepted 3 August 2010; published 26 October 2010)

Wettability is one of the surface characteristics that is controlled by the chemical composition and roughness of a surface. A number of investigations have explored the relationship between water contact angle and surface free energy of polymeric coatings with the settlement (attachment) and adhesion strength of various marine organisms. However, the relationship between the contact angle hysteresis and fouling-release property is generally overlooked. In the present work, coatings were prepared by using commercial hydrophobic homopolymer and copolymer polyolefins, which have nearly the same surface free energy. The effects of contact angle hysteresis, wetting hysteresis, and surface free energy on the fouling-release properties for sporelings of the green alga *Ulva* from substrates were then examined quantitatively under a defined shear stress in a water channel. The ease of removal of sporelings under shear stress from the polymer surfaces was in the order of PP > HDPE > PPPE > EVA-12 and strongly and positively correlated with contact angle and wetting hysteresis; i.e., the higher the hysteresis, the greater the removal. © 2010 American Vacuum Society. [DOI: 10.1116/1.3483467]

## I. INTRODUCTION

All surfaces immersed in the marine environment rapidly become fouled, thereby increasing roughness and hence frictional drag.<sup>1</sup> Surface free energy,<sup>2</sup> wettability,<sup>3</sup> mechanical properties,<sup>2</sup> and roughness<sup>4,5</sup> are the most important characteristics of a surface affecting its antifouling and fouling-release properties. Wettability is an important property of solid surfaces that determines surface characteristics and is controlled by the chemical composition and geometric microstructure of the surface. Recently, Genzer and Efimenko<sup>6</sup> investigated the relevance of superhydrophobic surfaces to marine fouling in a review. Roach *et al.*<sup>7</sup> reviewed the work on preparation of superhydrophobic surfaces, with focus on the different techniques used and how they have developed over the years and discussed the origins of water-repellent surfaces, examining how size and shape of surface features are used to control surface characteristics. Koch *et al.*<sup>8</sup> reviewed the description of cellular and subcellular plant surface structures, which include hairs, wax crystals, and surface folding where these structures and functions might be useful models for the development of functional materials. Others have noted the correlation between fouling deterrence and the structure of a number of marine organisms e.g., mussel shells,<sup>9–11</sup> although shell topography may not be the sole factor moderating deterrence<sup>12</sup> and not all natural surface topographies deter settlement.<sup>13,14</sup> The hydrophobicity of a substrate can be enhanced by adding controlled roughness and chemical modification. A number of investigations have

explored the relationship between water contact angle and surface free energy of polymeric substrates with the settlement (attachment) and/or adhesion strength of various marine organisms.<sup>15–21</sup> Generally, for a wide range of organisms, there is a good correlation between low surface energy of the coating and enhanced fouling-release performance (i.e., low adhesion strength), although there are exceptions, notably for marine diatoms, which adhere more strongly to hydrophobic surfaces.<sup>22</sup>

The green seaweed *Ulva* is the most common macroalgae that fouls man-made structures, including boats, buoys, ships, and submarines, and which reproduces by the production of vast numbers of microscopic motile spores (zoospores). Fouling is initiated by the settlement of the swimming spores, which then germinate to produce multicellular sporelings (young plants), which are attached to the substratum through uncharacterized adhesive materials released by the rhizoids (“rootlets”) of the developing seaweed. Sporelings of *Ulva* have been extensively used as a model system to evaluate the potential of surfaces as fouling-release coatings (see, e.g., Refs. 20 and 23–27).

Wettability of a liquid on a solid surface is determined by the contact angle analysis. When a liquid drop rests on a solid surface, it is in equilibrium by balancing three forces, namely, the interfacial tensions between solid and liquid, *SL*; that between solid and vapor, *SV*; and that between liquid and vapor, *LV*. Contact angle,  $\theta$ , is the angle formed by a liquid drop at the intersection point of three-phase boundary and it is included between the tangent plane to the surface of the liquid and the tangent plane to the surface of the

<sup>a)</sup>Electronic addresses: yerbil@gyte.edu.tr and yerbil19@yahoo.com

solid.<sup>28–30</sup> Contact angle is a quantitative measure of the wetting of a solid by a liquid and it is a manifestation of the thermodynamic equilibrium of the three-phase system so described. Low values of  $\theta$  indicate a strong liquid-solid interaction that the liquid tends to spread on the solid, or wets well, while high  $\theta$  values indicate weak interaction and poor wetting. In order to apply the thermodynamic equilibrium, the solid surface should be ideal: it must be chemically homogeneous, rigid, and flat at an atomic scale and is not perturbed by chemical interaction or by vapor or liquid adsorption. If such an ideal solid surface is present, there would be a single, unique contact angle. However, very few surfaces strictly adhere to this theory as a consequence of the non-ideal nature of any real surface. Surface roughness, chemical heterogeneity, swelling of the solid, liquid penetration, surface restructuring, and domain segregation are the main reasons for the measurement of different contact angle values on a surface. Experimentally, only two types of contact angle measurement technique are standardized: When a liquid drop is formed by injecting the liquid from a needle connected to a syringe, on a substrate surface, it is allowed to advance on the fresh solid surface and the measured angle is called as *advancing contact angle*,  $\theta_a$ . There is a maximum value of  $\theta_a$  before the three-phase line is broken for each drop-solid system. The other contact angle type is the *receding contact angle*,  $\theta_r$ , and it can be measured when a previously formed sessile drop on the substrate surface is contracted by applying a suction of the drop liquid through the needle.<sup>30</sup> The precise measurement of receding contact angles is a difficult process and  $\theta_r$  can be determined by following the time dependent drop evaporation measurements with a video-microscopy technique in comparison with the static needle-syringe sessile drop method.<sup>31,32</sup> Contact angle hysteresis, CAH, is defined as the difference between the advancing and receding contact angles,  $CAH \equiv \theta_a - \theta_r$ . This hysteresis is due to the system under investigation not meeting the ideal conditions.

The first report on the influence of CAH on the fouling resistance of the coatings toward marine fouling organisms was performed by Schmidt *et al.*<sup>33</sup> They investigated the relationship between CAH of a range of perfluoroalkyl coatings, where the adhesive properties of the coatings determined by peel fracture energies using pressure-sensitive adhesive tape, and the fouling resistance of the coatings toward marine fouling organisms, assessed through field exposures. The authors reported that the adhesive release properties of the coatings did not correlate well with the surface energies estimated from the static and advancing contact angles nor with the amount of fluorine present on the surface, but did show a correlation with water receding contact angles and cross-link density.<sup>33</sup> They reported that coatings having the best release properties had both the highest cross-link density and the lowest contact angle hysteresis. However, the assessment of resistance and ease of cleaning with respect to marine fouling performed by Schmidt *et al.*<sup>33</sup> were qualitative in nature and their intriguing observations demand further experimentation to validate their preliminary conclu-

sions. Therefore, we have conducted some controlled, quantitative experiments using polyolefinic homo- and copolymer coatings with a range of CAH values. For this purpose, we choose hydrophobic polymers which have nearly the same surface free energy in order to be able to investigate the CAH effect rather than independently from surface free energy. The fouling-release properties of these coatings have been examined quantitatively by investigating how easily sporelings of *Ulva* were released from coatings when exposed to hydrodynamic shear. A calibrated water-channel was used to remove sporeling biomass, which generates fully turbulent flow with a defined surface shear.<sup>34</sup>

Four types of polyolefins were used to prepare the test coatings for fouling-release experiments: polypropylene (PP), high density polyethylene (HDPE), polypropylene-polyethylene (PPPE) copolymer, and ethylene-vinyl acetate (EVA) copolymer. Polyolefins are a cheap class of plastics that can be used easily to prepare different types of surface coatings. Erbil *et al.*<sup>35</sup> proposed that superhydrophobic coatings could be generated simply and inexpensively through the use of PP homopolymer and selection of suitable solvents. We used the same phase-separation method given in Ref. 35 to produce our PP and high density polyethylene (HDPE) samples. HDPE is a commonly used plastic with a relatively simple chemical structure and well-known bulk properties. Its surface crystallinity can be changed by varying the process of coating formation. Thin HDPE films were produced by spin-coating technique and characterized by electron spectroscopy for chemical analysis, time-of-flight secondary ion mass spectrometry, optical microscopy, and atomic force microscopy (AFM).<sup>36</sup> Ethylene vinyl acetate (EVA) copolymers are produced by random copolymerization of ethylene and vinyl acetate monomers. EVA copolymers range from thermoplastic products, similar to PE, to rubberlike products at about 50% by weight of vinyl acetate (VAc). EVA is mainly recognized for its flexibility, toughness, and surface adhesion characteristics by varying the polar VAc content.<sup>37–40</sup>

In this study, surface coatings were prepared by dip-coating onto glass microscope slides from solutions of PP, HDPE, PPPE, and EVA-12 polymers dissolved in xylene. The release properties for young plants (sporelings) of a common marine fouling alga, *Ulva*, were investigated in terms of how contact angle hysteresis, wetting hysteresis, surface free energy, and surface morphology of these thin film coatings correlates to the ease of fouling release.

Our main objective is the investigation of the independent CAH effect on the removal of sporelings of *Ulva* by hydrodynamic shear stress produced in a water channel (expressed as % removal) from surfaces of these hydrophobic polymers which have very close surface free energy values, but large CAH differences.

## II. EXPERIMENT

### A. Materials

Polypropylene homopolymer (PP), was purchased from PETKIM, Turkey (PETOPLEN MH 418); ethylene-vinyl ac-

etate copolymer containing 12% vinyl acetate content by weight (EVA-12) was provided by Dupont (ELVAX 660); high density polyethylene homopolymer (HDPE) was provided from Basell Inc (HOSTALEN-GM8255) and polypropylene-polyethylene copolymer elastomer containing 12% polyethylene content by weight (PPPE) was purchased from Dow Chemical Co. (VERSIFY 2300). These polymers were used to prepare polymer solutions in xylene solvent (technical grade, TEKKIM, Turkey). Glass slides (ISOLAB, Turkey) were used as substrates and Milli-Q<sup>®</sup> water was used for the final cleaning of these glass slides. Two-component adhesive polyepoxide layer (404 Chemicals, Turkey) was used as the primer coating on glass slides.

## B. Polymer solutions and sample preparation

Standard glass slides (76×26 mm<sup>2</sup>) were initially cleaned in chromic acid, rinsed with distilled and Milli-Q<sup>®</sup> water, and dried in a vacuum oven. These slides were dip-coated with 404 adhesive polyepoxide layer from its chloroform solution as the primer coating to compensate for the weak adherence of polyolefines onto glass. PP, HDPE, PPPE, and EVA-12 polyolefins were dissolved in xylene between 60 and 130 °C to obtain solutions from 33.3 to 40.0 mg/ml (w/v). Polyepoxide coated glass slides were dip-coated in these polymer solutions at specific temperatures and dipping rates by using a mechanical dipper. Specific dipping solution temperatures were 102, 115, 100, and 105 °C for PP, HDPE, PPPE, and EVA-12 samples. Specific glass slide dipping rates were 77, 57, 360, and 612 mm/min for PP, HDPE, PPPE, and EVA-12 samples. Chemically heterogeneous surfaces having varying surface roughness were formed from copolymers by phase segregation during this controlled dip-coating and solvent evaporation process. Polymer-coated glass slides were dried in a vacuum oven overnight and kept in a desiccator until further experimentation.

## C. Water contact angle measurements

Contact angle measurements were carried out by using CAM 200 contact angle meter apparatus (KSV, Finland). Droplets (5 μl) of MERCK ultrapure grade water were formed on polymer films and equilibrium contact angles ( $\theta_e$ ) were determined immediately by using video frame grabbing method in order to prevent the drop evaporation errors.<sup>30</sup> The needle was removed from the droplet during  $\theta_e$  measurement. Advancing contact angles ( $\theta_a$ ) were measured when the droplet was expanding on the fresh surface by forming a 5 μl water droplet on a preformed 3 μl droplet. Receding contact angles ( $\theta_r$ ) were measured by slowly sucking 4–5 μl water from the preformed 8 μl droplet. The needle was kept within the droplet and 2 frames/s were recorded during the  $\theta_a$  and  $\theta_r$  measurements and these data were plotted against time by the software of the instrument. The maximum points were recorded as  $\theta_a$  values in the advancing contact angle-time plots and the minimum points were recorded as  $\theta_r$  in the receding contact angle-time plots. Drop evaporation experiments were also applied to the rough PP

and HDPE samples to obtain reliable  $\theta_r$  values.<sup>30–32</sup> Measurements were taken from at least three different locations on each sample (two coated samples of the same polymer type was used) and the reported values were the averages of at least 6 measurements. All the average contact angle results were within ±1°.

## D. Surface free energy

Equilibrium contact angles of water, ethylene glycol, formamide, methylene iodide, and  $\alpha$ -bromo naphthalene droplets were measured on all the substrates using spectroscopic grades of these liquids (MERCK). Van Oss–Good–Chaudhury methodology (acid-base approach) was used for the calculation of surface free energy of the samples.<sup>41,42</sup>

## E. Film thickness measurements

The thickness of the coated polymeric layers was measured by using a precise micrometer and also calculated from the weight increase of polymer films after coating.

## F. Optical and scanning electron microscopy

The surface topography of the coatings was examined by optical microscopy (Nikon SMZ 1500) up to 500× magnification. Scanning electron microscopy (SEM) images were obtained (Jeol JSM 7500TFE Model) in BASF-SE laboratories up to 10 000× magnification after sputter-coating with a 5 nm layer of gold-palladium.

## G. AFM in air and seawater

AFM experiments under ambient conditions (dry state) were done in the tapping mode on a commercial Multimode system equipped with a Nanoscope IIIa controller (Veeco Instruments) using silicon cantilevers with a nominal force constant of 42 N/m from Olympus (type OMCL-AC160TS) at a resonance frequency of about 320 kHz in BASF-SE. Laboratories. To analyze the behavior of the surfaces in a marine environment, artificial seawater (ASW) was prepared from Tropic Marin salt (Dr. Biener GmbH). Surfaces were stored in ASW for 7 days, and then transferred into the experimental chamber of the AFM filled with ASW, avoiding dry-out or surface reorganization. All *in situ* (in solution) experiments were conducted in the ac mode on a commercial MFP-3D system from Asylum Research using silicon cantilevers with an Al reflex coating and a nominal force constant of 2.8 N/m from Nanosensors (type PPP-FMR) at a resonance frequency of about 24 kHz. The scan rate was kept at 1 Hz in all experiments while the tip-sample forces were carefully minimized to avoid artifacts. Root-mean-square (rms) roughness values were determined over regions of 1 × 1 μm<sup>2</sup> size and averaged over at least 5 measurements.

## H. Biofouling and fouling-release determination

The removal of sporeling biomass from polyolefin surfaces followed the methods detailed in Beigbeder *et al.*<sup>25</sup> Briefly, surfaces were incubated with zoospores of *Ulva* for 1

h. After washing away swimming spores, the settled (attached) spores were allowed to germinate and grow for 6 days into small plants (sporelings). Sporeling biomass was determined prior to, and post the release step by *in situ* measurement of the fluorescence of chlorophyll, expressed as relative fluorescence units (RFU), by a plate reader (Tecan) (216 spot readings  $\times$  5 replicate surfaces were obtained for each polymer surface). The intensity of emitted light has been shown to scale linearly with the concentration of chlorophyll extracted in DMSO. Sporeling biomass was released, i.e., removed, by exposure to 51.5 Pa wall shear stress in a calibrated water-channel described in Ref. 34. The percentage removal of sporeling biomass was determined from the RFU values recorded before and after exposure to flow using 216 paired (before and after) readings per replicate slide. The removal was calculated for each of these individual points in the sporeling biofilm. Percentage removal data were arcsine transformed and the normality assessed using the Anderson–Darling test for conformity. Slides coated with polydimethyl siloxane (PDMS) (T2<sup>®</sup> Silastic) were included in the assay as standards as the properties of PDMS as fouling-release coatings for sporelings of *Ulva* are well documented.<sup>23,25,43</sup>

### III. THEORETICAL BASIS

#### A. Wetting hysteresis

It is common to find CAH on all practical nonideal surfaces, in the range of 10° or larger, and 50° or more of CAH has been recorded.<sup>42</sup> In general, surface roughness and the microscopic chemical heterogeneity of the solid surface are the most common causes of contact angle hysteresis, but it may also be caused by molecular reorientation on the polymer coating and drop size effects.<sup>30,42</sup> On the other hand, the wetting hysteresis, WH, is defined as the adhesion energy to cause CAH.<sup>28,29,44,45</sup>

$$WH = \gamma_{LV}(\cos \theta_r - \cos \theta_a), \quad (1)$$

where  $\gamma_{LV}$  is the surface tension of the liquid drop.

#### B. Determination of surface free energy

Van Oss *et al.* developed a more advanced approach than the geometric mean equation of Owens and Wendt,<sup>46</sup> which cannot be used when nonasymmetric hydrogen-bonding interactions are present, in order to estimate the surface free energy of solids from contact angles. Van Oss–Good–Chaudhury approach is based on the Lifshitz theory of the attraction between macroscopic bodies.<sup>41,42</sup> According to this approach, both the solid surface and liquid drop consists of two surface free energy component terms, one is  $\gamma_i^{LW}$  which is the “Lifshitz–van der Waals” component, comprising *dispersion*, *dipolar*, and *induction* interactions and the other term is  $\gamma_i^{AB}$  which is the “acid–base” component comprising all the electron donor–acceptor interactions, such as hydrogen-bonding. Their sum gives the total surface free energy. ( $\gamma_i^{tot} = \gamma_i^{LW} + \gamma_i^{AB}$ ). Van Oss–Good–Chaudhury proposed a three-parameter equation to calculate the surface free en-

ergy of solids when three liquid drops are used and their  $\gamma_L^{LW}$ ,  $\gamma_L^+$ , and  $\gamma_L^-$  values are known.

$$\gamma_{LV}(1 + \cos \theta) = 2(\sqrt{\gamma_S^{LW} \gamma_L^{LW}} + \sqrt{\gamma_S^+ \gamma_L^+} + \sqrt{\gamma_S^- \gamma_L^-}), \quad (2)$$

where subscript *S* is solid, *L* is liquid, *V* is vapor, superscript *LW* denotes the Lifshitz–van der Waals interactions, and *AB* denotes the acid–base interactions, ( $\gamma_i^{AB} = 2\sqrt{\gamma_i^+ \gamma_i^-}$ ), which can be calculated from Lewis acid,  $\gamma_i^+$ , and Lewis base,  $\gamma_i^-$  parameter of surface free energy. In order to apply Eq. (2) to the contact angle data, we need a set of values of  $\gamma_{LV}$ ,  $\gamma_L^{LW}$ ,  $\gamma_L^+$ , and  $\gamma_L^-$  for the reference liquids such as methylene iodide,  $\alpha$ -bromo naphthalene, ethylene glycol, glycerol, and formamide. Since  $\gamma_L^{LW} = \gamma_{LV}$  is for nonpolar liquids, the problem is to determine a set of  $\gamma_L^+$  and  $\gamma_L^-$  values for dipolar or monopolar liquids. Van Oss–Good introduced an arbitrary relation for water: They assumed that  $\gamma_W^+ = \gamma_W^-$  for water and since  $\gamma^{AB} = 51.0$  mJ/m<sup>2</sup> is known for water, then they calculated  $\gamma_W^+ = \gamma_W^- = 25.5$  mJ/m<sup>2</sup> from  $\gamma_i^{AB} = \gamma_i^{tot} - \gamma_i^{LW}$  and  $\gamma_i^{AB} = 2\sqrt{\gamma_i^+ \gamma_i^-}$ .<sup>41,42</sup> The values of all the acid–base parameters of test liquids derived from this approach were relative to those of water and finally they suggest a reference set of liquid surface free energy component data with these operational values, which are given in literature. In general, three forms of Eq. (2) are simultaneously solved by using the contact angle data of three different liquids with two of them being polar and hydrogen-bonding. Equilibrium contact angle values of these test liquids were used to calculate  $\gamma_S^{LW}$ ,  $\gamma_S^+$ ,  $\gamma_S^-$ ,  $\gamma_S^{AB}$ , and  $\gamma_S^{tot}$  results of the sample coatings by using Eq. (2). There are two possible methods to calculate the polymer surface unknown values of  $\gamma_S^{LW}$ ,  $\gamma_S^+$ , and  $\gamma_S^-$ . In the first method,  $\gamma_S^{LW}$  can be determined first by using only nonpolar liquids such as methylene iodide and  $\alpha$ -bromonaphthalene, and then the two other polar liquids are used to determine the  $\gamma_S^+$  and  $\gamma_S^-$  values. Sometimes negative square roots of  $\gamma_S^+$  and/or  $\gamma_S^-$  occur and it is recommended that if polar liquids are employed, water should always be used; otherwise, if only two polar liquids other than water are used (e.g., ethylene glycol and formamide), highly variable  $\gamma_S^+$  and  $\gamma_S^-$  values may be obtained.<sup>41,42</sup> In the second method, three forms of Eq. (2) are simultaneously solved by using the contact angle data of three different liquids with two of them being polar. In this work, we used water, methylene iodide (MeI<sub>2</sub>),  $\alpha$ -bromonaphthalene (Br-Naph), ethylene glycol (EG), and formamide (F) drops as test liquids, and we preferred the first calculation method and we determined the surface free energy component values by using an Excel spreadsheet which was previously prepared.

### IV. RESULTS AND DISCUSSION

#### A. Optical and scanning electron microscopies

The surface morphologies of the sample surfaces were determined by optical microscopy and SEM. The thickness of the coatings is dependent not only on the polymer type but also on the dipping solution temperature and the dipping rate. The thicknesses for PP and EVA-12 coatings were less than 1  $\mu$ m, for PPPE it was around 1.5–2.0  $\mu$ m, and for

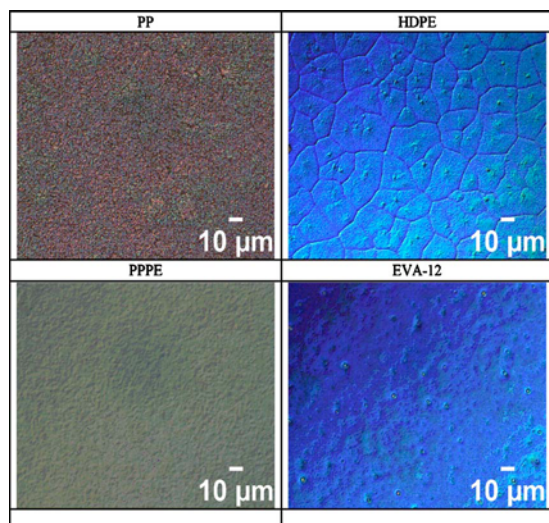


FIG. 1. (Color online) Optical microscope images of polyolefine surfaces (500 $\times$  magnification).

HDPE it was approximately 3  $\mu\text{m}$ . As seen in the optical microscopy images given in Fig. 1, the presence of large spherulites was seen only on HDPE coatings. SEM images of the same samples are given in Fig. 2. As seen in these images, microstructuring on the PP surface was due to semi-crystalline spherulitic structures, of typical dimensions 2–12  $\mu\text{m}$ , with some nanofibrillar structures. HDPE surfaces showed a large spherulitic texture and typical spherulite dimensions were 10–20  $\mu\text{m}$ , with some nanofibrillar structures having a dimension of 2–5  $\mu\text{m}$  at the center. PPPE surface was considerably flat when compared with other polyolefin surfaces. EVA-12 showed quite a homogeneous and flat surface where small protrusions (2–6  $\mu\text{m}$  in diameter) having slightly fibrillar structuring on a submicron scale were dispersed across the whole surface and there are large separation distances between them.

## B. AFM in air and AFM in seawater

PP and EVA-12 were studied by tapping mode AFM, before and after immersion in seawater (Figs. 3–5). Rms roughness values were determined from the amplitude images given in Fig. 3 as 76 nm for PP and 16 nm for EVA-12 under air. These values were changed by the contact with artificial seawater so that rms values increased to 80 nm for PP and 218 nm for EVA-12. The most important change was found for the EVA-12 sample as its rms increased more than 13 times due to the restructuring of the polar VAc groups in this copolymer surface when immersed in seawater. As seen in Figs. 3–5, surface structures were much coarsened after seawater contact for the PP sample. A strong moisture expansion was detected at the micron scale for the EVA-12 sample however the expansion at the nanometer-scale was not detectable. AFM-phase images given in Fig. 4 also show the soft (dark) and hard (bright) portions of these surfaces and in general all of the samples exhibited mainly a hard structure both in air and seawater. AFM-height images were also given

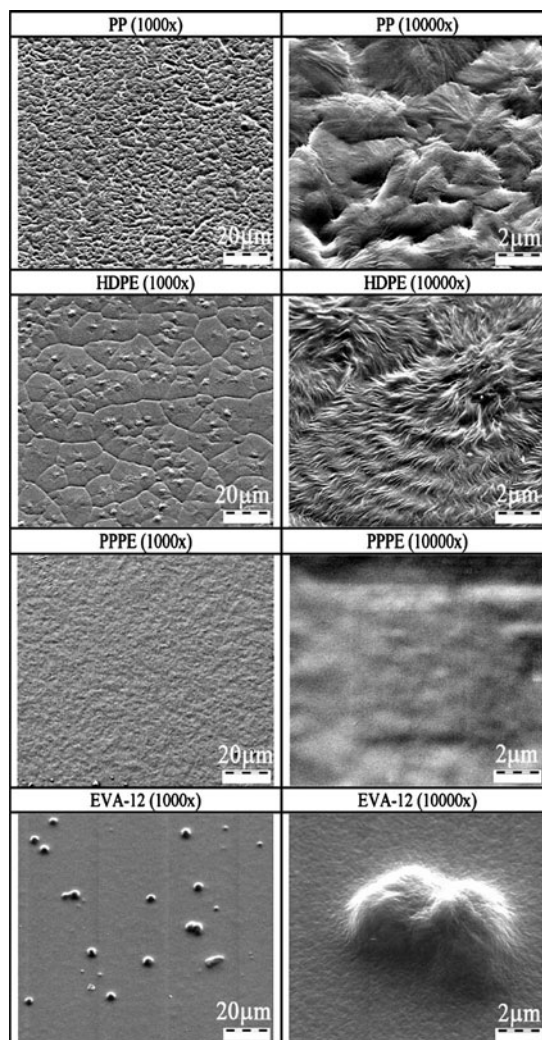


FIG. 2. SEM images of polyolefine surfaces.

in Fig. 5 for PP and EVA-12 samples in air and artificial sea water. Coarsening of the structures after immersion in seawater is also clearly seen in this figure.

## C. Water contact angles, wetting hysteresis, and polymer surface tension

Advancing, equilibrium, and receding contact angles of water drops, and resulting contact angle hysteresis values for each coating are given in Table I. The values of the WH were determined by using Eq. (1) and are also tabulated in Table I. It can be observed that water wettability was in the order EVA-12 > PPPE > HDPE > PP. Equilibrium contact angle values of the test liquids: methylene iodide ( $\text{MeI}_2$ ),  $\alpha$ -bromonaphthalene (Br-Naphth), ethylene glycol (EG), and formamide (F) drops were determined on sample surfaces and are given in Table II. These values were used to calculate  $\gamma_S^{\text{LW}}$ ,  $\gamma_S^+$ ,  $\gamma_S^-$ ,  $\gamma_S^{AB}$ , and  $\gamma_S^{\text{tot}}$  results of the substrates by using Eq. (2), and  $\gamma_S^-$  and  $\gamma_S^{\text{tot}}$  results are given in Table II.  $\gamma_S^{\text{tot}}$  values of PP, HDPE, and PPPE samples were close to each other ( $31.7 \pm 1.6 \text{ mJ/m}^2$ ) as expected from polyolefin polymers having only  $\text{CH}_2$  and  $\text{CH}_3$  groups. When all the

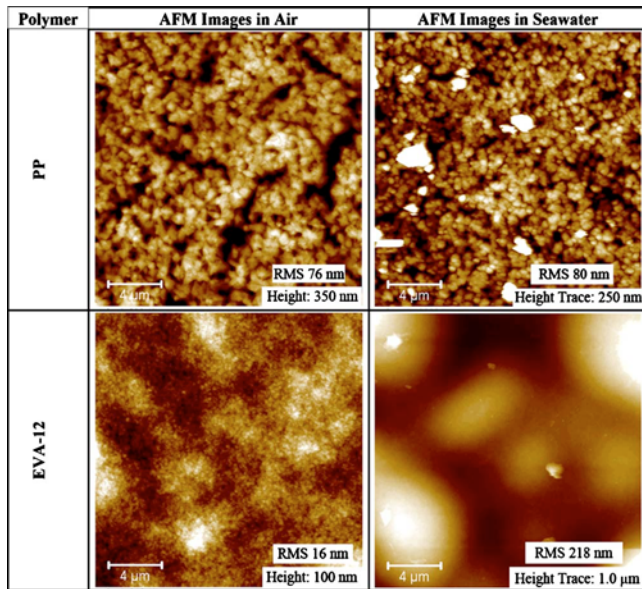


Fig. 3. (Color online) Amplitude AFM images of PP and EVA-12 in air and artificial seawater.

samples in Table II are considered, the mean  $\gamma_S^{\text{tot}} = 33.82 \pm 3.6$  mN/m and the variation of  $\gamma_S^{\text{tot}}$  for all the samples was only 10.6%. Nevertheless, since Eq. (2) was derived to be used for only flat surfaces, there are some inconsistencies for the  $\gamma_S^{\text{tot}}$  results of PP, HDPE, and PPPE polymers due to the formation of surface roughness on the coatings by phase separation during dip-coating.

The order of the surface roughness of the samples was PP > HDPE > PPPE > EVA-12, which was the inverse of their water wettability order.  $\gamma_S^{\text{tot}}$  value of EVA-12 was found to be 37.42 mJ/m<sup>2</sup>, which is around 20% higher than the other polyolefins due to the presence of polar and hydrogen-

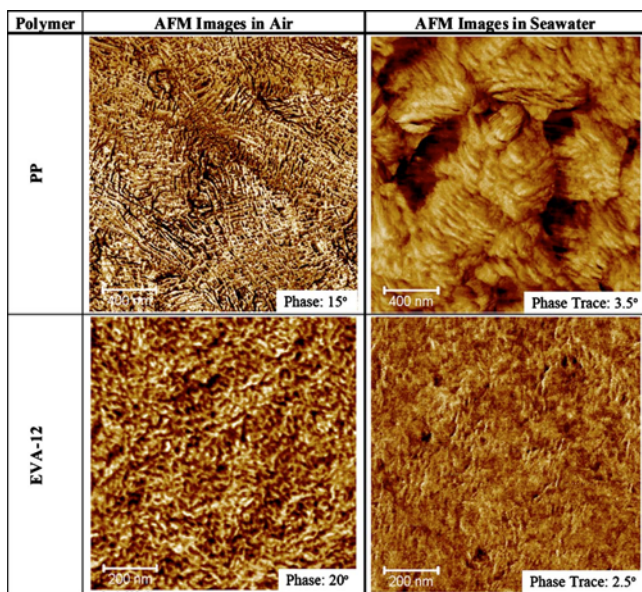


Fig. 4. (Color online) Phase AFM images of PP and EVA-12 in air and artificial seawater.

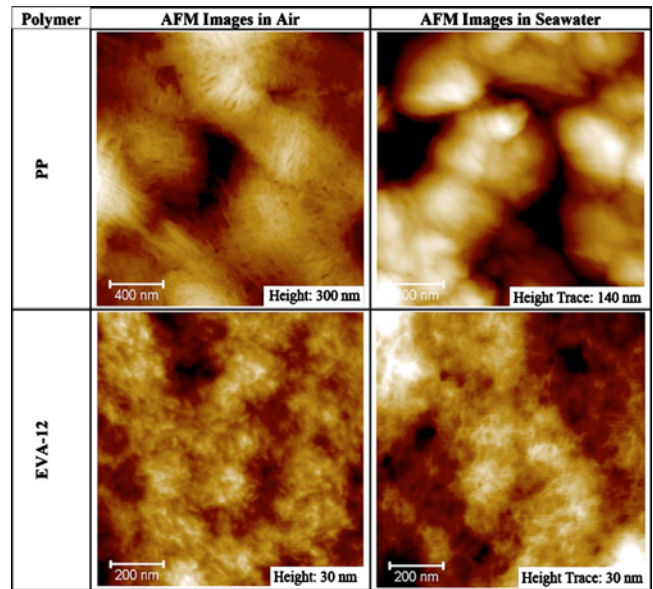


Fig. 5. (Color online) Height AFM images of PP and EVA-12 in air and artificial seawater.

bonding VA pendant groups on its surface. VA also increased the Lewis base surface free energy component ( $\gamma_S^-$ ) of EVA-12. In general, the increase of surface roughness on a hydrophobic coating results in a higher water contact angle, CAH, and WH values. Several examples of this behavior were reported in the literature.<sup>4,30,35</sup> Microstructuring on the PP surface due to formation of the semicrystalline spherulitic texture increased the equilibrium contact angle value of our PP sample up to 116° from the reported value of 106° (Ref. 35) for the flat PP surfaces. The equilibrium water contact angle on flat HDPE surfaces was reported around 100° (Ref. 42) and was measured as 107° on the dip-coated rough sample. Both contact angle hysteresis and wetting hysteresis were in the reverse order with the water wettability, so that PP had the highest and EVA-12 the lowest CAH and WH as seen in Table I. When all the samples are considered, the mean CAH = 28° ± 17° and the variation of CAH for all the samples was 60.7%. This is much larger than the variation of mean  $\gamma_S^{\text{tot}}$  which was 10.6% as calculated from Table II. This is in accordance with our intention to use hydrophobic polymers having very close surface free energy but large CAH in order to be able to investigate the CAH effect rather independently from surface free energy.

The extent of CAH depends on the surface roughness effect for the chemically homogeneous polymers such as PP, HDPE, and PPPE; the higher the roughness, the higher the CAH and WH were obtained. Surface roughness cause the pinning of water drop on the surface during the advancing contact angle measurement giving a rise in the CAH results. When EVA-12 sample is considered, it shows the lowest CAH result (11°) among all the substrates. The advancing contact angle is small (95°) when compared with the other substrates, which is a direct consequence of the strong interaction between EVA-12 surface having carbonyl groups and water. In addition, EVA-12 is the sample with the lowest

TABLE I. Contact angle, CAH, and WH results of water drops on the sample surfaces. Contact angles were measured in three different locations on each surface and the reported values were the averages of at least 6 measurements. All the average contact angle results varied within  $\pm 1^\circ$ . This corresponds to  $\pm 2^\circ$  for the contact angle hysteresis values.

Sample	$\theta_a$ (deg)	$\theta_e$ (deg)	$\theta_r$ (deg)	CAH= $\theta_a - \theta_r$ (deg)	WH (mJ/m <sup>2</sup> )
PP	123	116	78	45	54.8 $\pm$ 2.3
HDPE	112	107	77	35	43.6 $\pm$ 2.4
PPPE	107	105	83	24	30.2 $\pm$ 2.5
EVA-12	95	93	84	11	14.0 $\pm$ 2.5

roughness as seen from its SEM images (Fig. 2). The bumps present on the EVA-12 surface do not have sharp edges which are necessary for a strong pinning. So, the receding contact angle ( $84^\circ$ ) is not much smaller than the advancing contact angle giving the lowest CAH result.

#### D. Relationship between adhesion strength of sporelings of *Ulva* and surface properties of the substrates

A green lawn of sporelings (young plants) covered the surface of all of the test samples after culturing for 6 days. Fouling-release performance of the coatings was assessed by measuring the proportion of the sporeling biomass removed under a defined wall shear stress of 51.5 Pa in a water channel, as reported in Table III. Percentage removal differed between the various polymers. The trend of removal from the homopolymers was in the reverse order to their relative wettabilities quantified by their equilibrium water contact angles. Sporelings showed higher removal from hydrophobic surfaces and PP showed the best fouling-release properties and EVA-12 the lowest, as given in Fig. 6. This is in agreement with the results of Gudipati *et al.*<sup>26</sup> and Krishnan *et al.*<sup>27</sup> where the strength of attachment of sporelings was typically lower on the hydrophobic surfaces.

When the relationship between contact angle hysteresis and sporeling removal is considered, the average removal of sporelings from the polyolefin surfaces showed a strong and positive trend with CAH and WH in our work, i.e., the higher the contact angle and wetting hysteresis, the greater the removal, as given in Figs. 7 and 8, respectively. There was a strong positive relationship ( $R^2$  of trend-line=0.9862 between the average removal of sporelings versus CAH in Fig. 7 and  $R^2=0.9911$  between the average removal of

sporelings versus WH in Fig. 8. Figures 7 and 8 show similar trends of the effect of contact angle and wetting hysteresis on the *Ulva* removal %. However, Fig. 8 shows the improvement of the linearity of the *Ulva* removal data when wetting hysteresis is used rather than the contact angle hysteresis. Our experimental findings also agree with other reported observations of sporelings of *Ulva* removal % with CAH given in the literature. Yarbrough *et al.*<sup>24</sup> reported that the removal of *Ulva* sporelings from poly (MMA-co-GMA-g-PFPEd) terpolymer having a CAH of  $24^\circ$  was larger than the poly (MMA-co-GMA-g-PFPEM) terpolymer having a CAH of  $20^\circ$ . Gudipati *et al.*<sup>26</sup> reported that for their samples synthesized from cross-linked hyperbranched fluoropolymer (HBFP) and poly(ethylene glycol) (PEG) amphiphilic networks, their sample coded as HBFP-PEG45 having a CAH value of  $30^\circ \pm 6^\circ$  resulted in the 40% removal, whereas sample HBFP-PEG55 having a CAH value of  $25^\circ \pm 10^\circ$  resulted in 10% removal, showing that the higher the mean CAH, the higher the spore removal for these chemically heterogeneous samples. HBFP-PEG45 sample surface also resulted in the largest removal of 8 days old sporelings.

Krishnan *et al.*<sup>27</sup> reported that high levels of CAH were positively correlated with ease of removal from coatings synthesized from polystyrene-polyisobutylene block copolymers with fluorinated side-chains. Their samples coded as poly(dimethylsiloxane) (PDMS) having a CAH value of  $46^\circ \pm 6^\circ$  resulted in 80% *Ulva* sporeling removal, block copolymer sample (27/13)F10H9 having a CAH value of  $38^\circ \pm 4^\circ$  resulted in 45% sporeling removal, and polystyrene-block-poly(ethylene-ran-butylene)-block-polystyrene (SEBS) having a CAH value of  $35^\circ \pm 2^\circ$  resulted in 27% removal. All these results show that the higher the CAH, the higher the *Ulva* sporeling removal for these samples (we did not con-

TABLE II. Equilibrium contact angle results of test liquid drops and the calculated surface free energy values. Contact angles were measured in three different locations on each sample surface and the reported values were the averages of at least 6 measurements. All the average contact angle results varied within  $\pm 1^\circ$ .

Sample	$\theta_{Me12}$ (deg)	$\theta_{Br-Naph}$ (deg)	$\theta_F$ (deg)	$\theta_{EG}$ (deg)	$\gamma_s^-$ (mJ/m <sup>2</sup> )	$\gamma^{tot}$ (mJ/m <sup>2</sup> )
PP	59	45	76	74	0	31.08
HDPE	54	41	83	68	0	33.45
PPPE	56	52	88	77	0.07	30.22
EVA-12	48	30	73	67	1.38	37.42

TABLE III. Mean percentage removal ( $\pm 2 \times$  standard error) of sporeling biomass of *Ulva* from test surfaces by 51.5 Pa wall shear stress in the water flow-channel apparatus. Each value represents the mean of 5 replicates, calculated from 216 paired readings (before and after exposure to flow) per replicates test surface. The  $2 \times$  standard error was calculated from arcsine-transformed data. Mean percentage removal from the PDMS (T2 Silastic) standard was 22.4%.

Sample	Removal %
PP	35.3 $\pm$ 0.9
HDPE	31.3 $\pm$ 0.6
PPPE	23.8 $\pm$ 0.6
EVA-12	14.2 $\pm$ 1.3

sider block copolymer sample (10/12)F10H9 having a CAH value of  $37^\circ \pm 4^\circ$  resulted in 70% removal in this trend analysis since both (10/12)F10H9 and (27/13)F10H9 samples have nearly the same CAH but very different removal results). Lee *et al.*<sup>47</sup> reported sporeling removal from the coatings obtained from the phenol-catalyzed cross-linking of 1,9-bis(glycidyoxypropyl) decamethylpentasiloxane: the higher the CAH of the substrate, the higher the removal of sporelings.

To the best of our knowledge, only Schmidt *et al.*<sup>33</sup> investigated the relationship between CAH of perfluoroalkyl coatings, with the fouling resistance toward marine fouling organisms assessed in this case through field exposures. These authors reported that coatings having the best release properties had the lowest contact angle hysteresis, a conclusion that is the opposite of our findings. Two possible reasons for this difference are the following: (1) the assessment of resistance and ease of cleaning with respect to marine fouling performed by Schmidt *et al.*<sup>33</sup> was qualitative in nature and was performed on complex multiorganism fouling communities rather than defined organisms under controlled conditions; (2) they preferred to use only sinus of the tilt angles to quantify CAH depending on the ‘‘Furmidge equation’’<sup>48</sup> although they measured both advancing and receding contact angles. When CAH is recalculated from their data as the

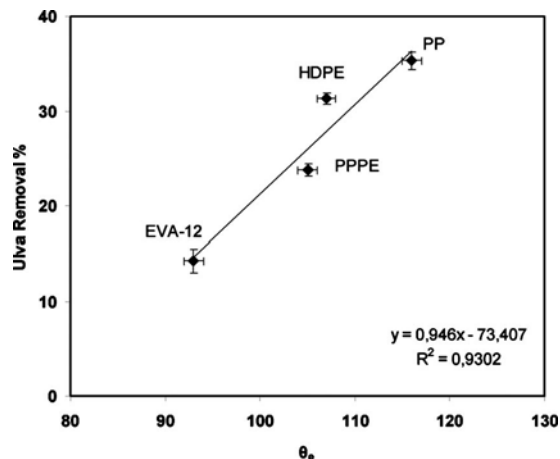


FIG. 6. Removal % of *Ulva* plotted against with the change of the equilibrium water contact angle variation.

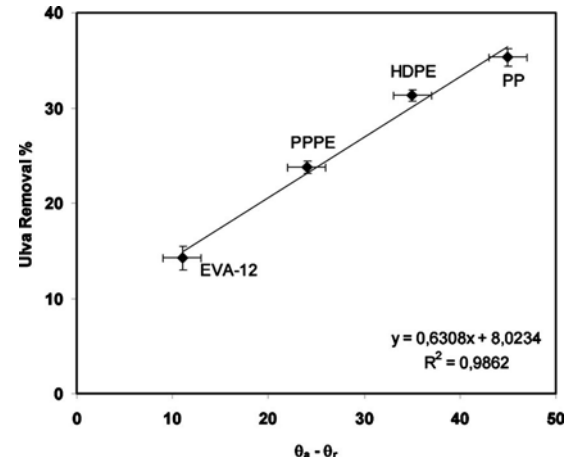


FIG. 7. Removal % of *Ulva* plotted against the water contact angle hysteresis.

difference between advancing and receding contact angles, as its definition implies, then there is no correlation of bio-fouling data with the contact angle hysteresis results given in Ref. 33. The Furmidge equation was derived by considering the mechanical equilibrium conditions for liquid droplets on tilted surfaces in a gravity field:

$$mg \sin \phi = \omega \gamma_L (\cos \theta_r - \cos \theta_a), \quad (3)$$

where  $m$  is the mass of the drop,  $g$  is the acceleration of gravity,  $\phi$  is the tilt angle of the plane with respect to the horizontal,  $\gamma_L$  is the surface tension of the liquid,  $\theta_a$  and  $\theta_r$  are the advancing and receding angles, respectively, and  $\omega$  is the width of the drop along a line parallel to the plane and perpendicular to its maximum inclination direction.<sup>48</sup> The equation predicts the minimum  $\phi$  angle at which a droplet will spontaneously move. However, there are practical and theoretical problems with this equation: from the practical side, the use of tilting plates to determine both the receding and advancing contact angles was negatively criticized in some previous publications.<sup>31,42</sup> Good<sup>42</sup> cautioned against this method because it yields values of advancing and reced-

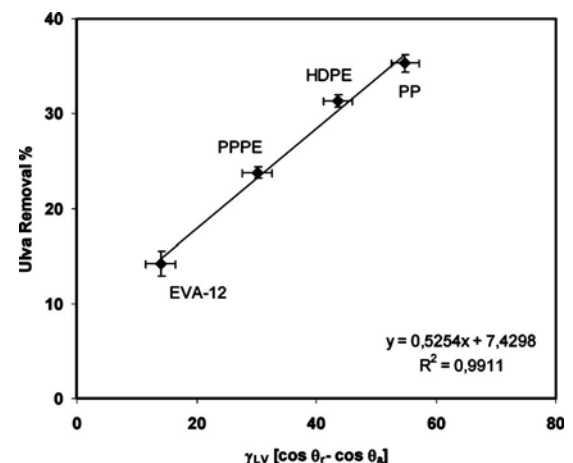


FIG. 8. Removal % of *Ulva* plotted against the water wetting hysteresis.

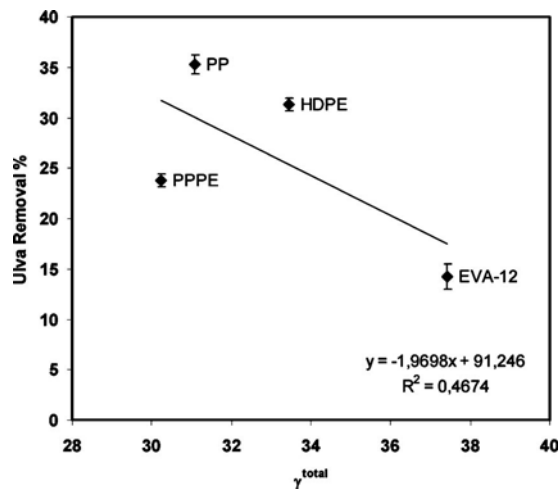


FIG. 9. Removal % of *Ulva* plotted against the substrate's total surface free energy,  $\gamma^{\text{total}}$ .

ing angles that are strongly dependent on the drop size. From the theoretical point of view, when a droplet moves on a surface, only solid-liquid interfacial water molecules that move are those on the contact line according to the no-slip boundary condition of fluid mechanics. On most materials, a droplet placed on the surface will come to rest at a local energy minimum (due to either chemical structure or topography), the contact line will be fixed, and there will be energy barriers for advancing and receding; these are the causes of hysteresis. Gao and McCarthy<sup>49,50</sup> reported that the advancing, receding contact angles, and CAH are determined by interactions of the liquid and solid at the three-phase contact line alone and the interfacial area within the contact perimeter is irrelevant. In a recent article, Yang *et al.*<sup>51</sup> investigated the effect of upper contact line on the sliding behavior of water droplet on superhydrophobic surface and concluded that the sliding angle is merely determined by the length of upper contact line, and it is irrelevant to the state of interfacial area of solid-water and lower contact line. Apart from all of these arguments, since the definition of CAH =  $\theta_a - \theta_r$ , then the use of tilt angles in Furmidge equation to determine CAH value, while both  $\theta_a$  and  $\theta_r$  values are known, is unreasonable and the conclusions reached in Ref. 33 are questionable.

However, when the total surface free energies of the polymeric coatings are considered, there is a weak inverse relationship between  $\gamma_s^{\text{tot}}$  and removal %, as seen in Fig. 9. This shows that surface roughness and chemical heterogeneity which can be expressed by the CAH results are more important factors than the surface free energy of the same substrate in order to understand foul-release properties from these surfaces. Since CAH is caused by two independent effects, which are surface roughness and chemical heterogeneity, it is not appropriate to attribute a single reason to increase the sporeling of *Ulva* release from surfaces at present. This needs further research by keeping the importance of CAH effect in mind during the fouling-release tests.

## V. SUMMARY AND CONCLUSIONS

In this contribution, we have demonstrated the preparation of polyolefinic PP, HDPE, PPPE, and EVA-12 films having close surface free energies by dip-coating and the fouling-release properties of these films have been examined quantitatively by investigating how easily sporelings of *Ulva* are released from film surfaces when exposed to hydrodynamic shear. The percentage of removal of sporelings is evaluated in terms of a variety of contact angle hysteresis, wetting hysteresis, surface free energy, and surface morphology of these thin film coatings. It was determined that *Ulva* sporelings showed higher removal from hydrophobic surfaces in agreement with the previously published results and PP showed the best fouling-release properties and EVA-12 the lowest. However, in contrast with a previous report,<sup>33</sup> the ease of removal of sporelings under shear stress from the polymer surfaces was strongly and positively correlated with contact angle and wetting hysteresis, i.e., the higher the hysteresis, the greater the removal and in the order of PP > HDPE > PPPE > EVA-12. This finding was also supported with the results of some recent reports.<sup>24,26,27,47</sup> Only a weak inverse relationship between  $\gamma_s^{\text{tot}}$  of the polyolefinic films and *Ulva* removal was found showing that contact angle hysteresis results are the more important parameter than the surface free energy of the films in order to correlate with the *Ulva* foul-release properties from these surfaces.

## ACKNOWLEDGMENTS

The authors gratefully acknowledge the support from the EC-Sixth Framework Integrated Project-AMBIO "Advanced Nanostructured Surfaces for the Control of Biofouling," Project No. NMP4-CT-2005-011827. The authors gratefully acknowledge their AMBIO project partner, BASF-SE, for the SEM and AFM images.

- <sup>1</sup>M. P. Schultz, *Biofouling* **23**, 331 (2007).
- <sup>2</sup>R. F. Brady and I. L. Singer, *Biofouling* **15**, 73 (2000).
- <sup>3</sup>M. E. Callow, J. A. Callow, L. K. Ista, S. E. Coleman, A. C. Nolasco, and G. P. Lopez, *Appl. Environ. Microbiol.* **66**, 3249 (2000).
- <sup>4</sup>J. Genzer and J. Groenewold, *Soft Matter* **2**, 310 (2006).
- <sup>5</sup>J. F. Schumacher, M. L. Carman, T. G. Estes, A. W. Feinberg, L. H. Wilson, M. E. Callow, J. A. Callow, J. A. Finlay, and A. B. Brennan, *Biofouling* **23**, 55 (2007).
- <sup>6</sup>J. Genzer and K. Efimenko, *Biofouling* **22**, 339 (2006).
- <sup>7</sup>P. Roach, N. J. Shirtcliffe, and M. I. Newton, *Soft Matter* **4**, 224 (2008).
- <sup>8</sup>K. Koch, B. Bhushan, and W. Barthlott, *Soft Matter* **4**, 1943 (2008).
- <sup>9</sup>A. V. Bers and M. Wahl, *Biofouling* **20**, 43 (2004).
- <sup>10</sup>A. J. Scardino, J. Guenther, and R. de Nys, *Biofouling* **24**, 45 (2008).
- <sup>11</sup>A. J. Scardino, D. Hudleston, Z. Peng, N. A. Paul, and R. de Nys, *Biofouling* **25**, 83 (2009).
- <sup>12</sup>A. V. Bers *et al.*, *Biofouling* **26**, 367 (2010).
- <sup>13</sup>J. Guenther, G. Walker-Smith, A. Waren, and R. de Nys, *Biofouling* **23**, 413 (2007).
- <sup>14</sup>J. Guenther and R. de Nys, *Biofouling* **23**, 419 (2007).
- <sup>15</sup>R. F. Brady, *Prog. Org. Coat.* **35**, 31 (1999).
- <sup>16</sup>R. F. Brady and C. L. Aronson, *Biofouling* **19**, 59 (2003).
- <sup>17</sup>L. Hoipkemeier-Wilson, J. F. Schumacher, M. L. Carman, A. L. Gibson, A. W. Feinberg, M. E. Callow, J. A. Finlay, J. A. Callow, and A. B. Brennan, *Biofouling* **20**, 53 (2004).
- <sup>18</sup>J. A. Callow, M. E. Callow, L. K. Ista, G. Lopez, and M. K. Chaudhury, *J. R. Soc., Interface* **2**, 319 (2005).
- <sup>19</sup>M. L. Carman, T. G. Estes, A. W. Feinberg, J. F. Schumacher, W. Wilk-

- erson, L. H. Wilson, M. E. Callow, J. A. Callow, and A. B. Brennan, *Biofouling* **22**, 11 (2006).
- <sup>20</sup>P. Majumdar *et al.*, *Biofouling* **24**, 185 (2008).
- <sup>21</sup>A. J. Scardino, H. Zhang, D. J. Cookson, R. N. Lamb, and R. deNys, *Biofouling* **25**, 757 (2009).
- <sup>22</sup>R. Holland, T. M. Dugdale, R. Wetherbee, A. B. Brennan, J. A. Finlay, J. A. Callow, and M. E. Callow, *Biofouling* **20**, 323 (2004).
- <sup>23</sup>M. K. Chaudhury, J. A. Finlay, J. Y. Chung, M. E. Callow, and J. A. Callow, *Biofouling* **21**, 41 (2005).
- <sup>24</sup>J. C. Yarbrough, J. P. Rolland, J. M. DeSimone, M. E. Callow, J. A. Finlay, and J. A. Callow, *Macromolecules* **39**, 2521 (2006).
- <sup>25</sup>A. Beigbeder, P. Degee, S. L. Conlan, R. J. Mutton, A. S. Clare, M. E. Pettitt, M. E. Callow, J. A. Callow, and P. Dubois, *Biofouling* **24**, 291 (2008).
- <sup>26</sup>C. S. Gudipati, J. A. Finlay, J. A. Callow, M. E. Callow, and K. L. Wooley, *Langmuir* **21**, 3044 (2005).
- <sup>27</sup>S. Krishnan *et al.*, *Biomacromolecules* **7**, 1449 (2006).
- <sup>28</sup>R. J. Good, *J. Am. Chem. Soc.* **74**, 5041 (1952).
- <sup>29</sup>Y. L. Chen, C. A. Helm, and J. N. Israelachvili, *J. Phys. Chem.* **95**, 10736 (1991).
- <sup>30</sup>H. Y. Erbil, *Surface Chemistry of Solid and Liquid Interfaces* (Blackwell, Oxford, UK, 2006), Chap. 9, pp. 308–337.
- <sup>31</sup>H. Y. Erbil, G. McHale, S. M. Rowan, and M. I. Newton, *Langmuir* **15**, 7378 (1999).
- <sup>32</sup>H. Y. Erbil, *J. Phys. Chem. B* **102**, 9234 (1998).
- <sup>33</sup>D. L. Schmidt, R. F. Brady, K. Lam, D. C. Schmidt, and M. K. Chaudhury, *Langmuir* **20**, 2830 (2004).
- <sup>34</sup>M. P. Schultz, J. A. Finlay, M. E. Callow, and J. A. Callow, *Biofouling* **15**, 243 (2000).
- <sup>35</sup>H. Y. Erbil, A. L. Demirel, Y. Avci, and O. Mert, *Science* **299**, 1377 (2003).
- <sup>36</sup>O. Mellbring, S. K. Øiseth, A. Krozer, J. Lausmaa, and T. Hjertberg, *Macromolecules* **34**, 7496 (2001).
- <sup>37</sup>A. M. Henderson, *IEEE Electr. Insul. Mag. (USA)* **9**, 30 (1993).
- <sup>38</sup>H. Y. Erbil, *J. Appl. Polym. Sci.* **33**, 1397 (1987).
- <sup>39</sup>M. Brogly, M. Nardin, and J. Schultz, *J. Appl. Polym. Sci.* **64**, 1903 (1997).
- <sup>40</sup>J. Kim, J. Wang, H. J. Kang, and F. Talke, *Polym. Eng. Sci.* **48**, 277 (2008).
- <sup>41</sup>C. J. Van Oss, M. K. Chaudhury, and R. J. Good, *Chem. Rev.* **88**, 927 (1988).
- <sup>42</sup>R. J. Good, in *Contact Angle Wettability and Adhesion*, edited by K. L. Mittal (VSP, Utrecht, 1993), pp. 3–36.
- <sup>43</sup>J. A. Finlay, B. R. Fletcher, M. E. Callow, and J. A. Callow, *Biofouling* **24**, 219 (2008).
- <sup>44</sup>M. K. Chaudhury and M. J. Owen, *J. Phys. Chem.* **97**, 5722 (1993).
- <sup>45</sup>C. W. Extrand and Y. Kumagai, *J. Colloid Interface Sci.* **191**, 378 (1997).
- <sup>46</sup>D. K. Owens and R. C. Wendt, *J. Appl. Polym. Sci.* **13**, 1741 (1969).
- <sup>47</sup>N. S. Lee, J. A. Callow, M. E. Callow, J. A. Finlay, and W. P. Weber, *J. Appl. Polym. Sci.* **102**, 751 (2006).
- <sup>48</sup>C. G. L. Furnidge, *J. Colloid Sci.* **17**, 309 (1962).
- <sup>49</sup>L. Gao and T. J. McCarthy, *Langmuir* **23**, 3762 (2007).
- <sup>50</sup>L. Gao and T. J. McCarthy, *Langmuir* **24**, 9183 (2008).
- <sup>51</sup>C. W. Yang, P. F. Hao, and F. He, *Chin. Sci. Bull.* **54**, 727 (2009).